rapid communication

Cardiomyocyte DNA synthesis and binucleation during murine development

MARK H. SOONPAA, KYUNG KEUN KIM, LAURA PAJAK, MICHAEL FRANKLIN, AND LOREN J. FIELD
Krannert Institute of Cardiology, Indiana University School of Medicine, Indianapolis, Indiana 46202-4800

Soonpaa, Mark H., Kyung Keun Kim, Laura Pajak, Michael Franklin, and Loren J. Field. Cardiomyocyte DNA synthesis and binucleation during murine development. *Am. J. Physiol.* 271 (*Heart Circ. Physiol.* 40): H2183–H2189, 1996.—Cardiomyocyte DNA synthesis and binucleation indexes were determined during murine development. Cardiomyocyte DNA synthesis occurred in two temporally distinct phases. The first phase occurred during fetal life and was associated exclusively with cardiomyocyte proliferation. The second phase occurred during early neonatal life and was associated with binucleation. Collectively, these results suggest that cardiomyocyte reduplication ceases during late fetal life. Northern and Western blot analyses identified several candidate genes that were differentially expressed during the reduplicative and binucleation phases of cardiomyocyte growth.

cardiomyocyte reduplication; cell cycle regulation

THE HEART is one of the first organs to develop during embryogenesis. Cardiac progenitor cells arise from a region of the splanchnic mesenchyme ventral to the pericardial coelom (17). After the initial commitment to the cardiogenic lineage, the tubular heart is formed. This structure subsequently elongates and forms alternate dilatations and contractions that give rise to the truncus arteriosus, bulbus cordis, ventricles, atria, and sinus venosus. Heart organogenesis culminates with the formation of a four-chambered structure with well-developed conduction and circulatory systems. Cardiomyocyte terminal differentiation is thought to occur shortly after birth in most mammals and is characterized by a transition from hyperplastic to hypertrophic growth. At the morphological level, this transition is accompanied by a marked increase in myofibril density, the maturation of intercellular junctional complexes (intercalated discs), and the appearance of binucleated cells. After this terminal differentiation process, increases in heart muscle mass arise as a consequence of hypertrophic cardiomyocyte growth in the absence of cell division.

Although the molecular basis of cardiomyocyte terminal differentiation remains unknown, it is likely that this process is both highly redundant and essentially irreversible. This view is supported by the rarity of primary myocardial tumors in adults as well as by the paucity of cardiomyocyte DNA synthesis in either normal or injured adult hearts (9, 17, 19). Identification of the key molecular regulators of cardiomyocyte terminal differentiation requires a working knowledge of the precise temporal pattern of cell cycle withdrawal and binucleation. Previous studies have shown that cardiomyocyte binucleation occurs during early neonatal life in both mice and rats (2, 4, 17). These studies documented a gradual decrease in radiolabeled thymidine incorporation that was coincident with the appearance of binucleated cells. This observation led to the suggestion that binucleation arises as a consequence of karyokinesis in the absence of cytokinesis.

In this report, the temporal pattern of cardiomyocyte cell cycle withdrawal and binucleation was characterized in inbred mice. Unexpectedly, cardiomyocyte DNA synthesis was observed to occur in two temporally distinct phases during murine development. The first phase of DNA synthesis occurred in fetal life and was associated exclusively with cardiomyocyte proliferation (reduplication). The second phase of cardiomyocyte DNA synthesis occurred in neonatal life and was associated predominately with binucleation. This suggests that cardiomyocyte reduplication ceases before birth in mice, and that the key gene products regulating proliferation would likely be expressed differentially during fetal versus neonatal life. Northern and Western blot surveys identified several genes with potential roles in the regulation of the cardiomyocyte cell cycle; these genes were expressed differentially during the reduplication versus binucleation phases of cardiomyocyte DNA synthesis. These observations are discussed with respect to the potential for regenerative cardiomyocyte growth in the adult heart.

METHODS

Cardiomyocyte DNA synthesis and binucleation assay. Experimental mice (C3Heb/FeJ, Jackson Laboratory, Bar Harbor, ME) were given a single injection of tritiated thymidine (200 μCi ip at 28 Ci/mM; Amersham, Arlington Heights, IL). To prevent nutrition-related variation in neonatal animals, all litter sizes were adjusted (6 pups/litter). Four animals were analyzed at each time point. Cardiomyocytes were prepared after a 2-h labeling period. Animals were administered heparin (10 ml/kg ip; Sigma Chemical, St. Louis, MO) and killed by cervical dislocation. Body weight was determined, and the hearts were removed and placed in a beaker of

phosphate-buffered saline (PBS). For neonatal and adult mice, isolated cardiomyocytes were prepared by retrograde perfusion with collagenase as described previously (19). For fetal mice, hearts were harvested, minced, and incubated in 0.17% collagenase at 37°C for 45 min, then triturated. Cell suspensions were placed in several volumes of 10% neutral buffered Formalin. After fixation, the cell suspensions were filtered through a fine mesh to remove tissue chunks, then smeared onto positively charged slides (Superfrost Plus, Fisher, Pittsburgh, PA), and allowed to dry.

For autoradiography, slides of isolated cardiomyocytes were washed with PBS, stained with 4′,6-diamidino-2-phenylindole (DAPI) in PBS (0.28 μM, 3 min at room temperature; Boehringer Mannheim, Indianapolis, IN), and washed 3 times in PBS. After drying was completed, stained slides were coated with photographic emulsion (Ilford L.4, Polysciences, Warrington, PA), diluted 1:1 with H_2O, drained, and placed in a light-tight box for 1 wk at 4°C. Slides were then developed in Kodak D-19 (Kodak, Rochester, NY) for 4 min, washed in H_2O, and fixed in 30% sodium thiosulfate for ≥4 min. Slides were further processed by washing in H_2O and by dehydration through graded ethanols and xylene, followed by application of a coverslip. Labeling indexes and nuclear counts were determined using a Leitz fluorescent microscope with a ×40 objective. Counting cells that appeared to be intact and separate was initiated in one corner of the slide and continued in length-wise rows. All results are expressed as means ± SE. A group *t*-test was employed for statistical analyses.

RNA isolation and Northern blot analyses. Hearts were homogenized with a Polytron in 4.0 M guanidinium thiocyanate, 1% β-mercaptoethanol, and RNA purified by centrifugation through 5.7 M CsCl as described (18). RNA samples were quantitated by spectrophotometry at 260 nm. For Northern analysis, RNA (10 μg) was denatured with glyoxal, separated by size on 1.2% agarose gels, and transferred to Genescreen (Du Pont, Wilmington, DE). Probes were radiolabeled by the nick translation method (18). Specific activities of the probes were typically $2–3 \times 10^9$ dpm/μg. Hybridizations were for 20 h at 65°C in 4 × standard saline citrate (SSC), 2 × Denhardt's, 0.1% sodium dodecyl sulfate (SDS), and 1 mg/ml salmon sperm DNA. Blots were washed at 65°C in 2 × SSC and 0.1% SDS and signal visualized by autoradiography at −70°C with an intensifying screen. The cDNA probes used in this study were p107 (nucleotide residues 890–1260, see Ref. 12), p53 (nucleotide residue 1060–1580; see Ref. 14), Gax (growth-arrest specific homeobox; nucleotide residues 274–649; see Ref. 6), TSC2 (tuberous sclerosis complex 2; nucleotide residues 1–5100; see Ref. 10), and ANF (atrial natriuretic factor; nucleotide residues 1–910; see Ref. 1). Quality of the RNA samples was confirmed by Northern analysis with a murine 18s rRNA oligonucleotide probe (5′-TCCATTATTCCTAGTGCGGTATCCAGGAGGATCGGGCCTGCTTT-3′; see Ref. 16).

Protein isolation and Western blot analyses. Hearts were homogenized directly in Nonidet P-40 buffer [150 mM NaCl, 5 mM EDTA, 50 mM tris(hydroxymethyl)aminomethane·HCl pH 8.0, 1 μg/ml aprotinin, 1 μg/ml pepstatin, 1 μg/ml leupeptin, 50 μg/ml *N*α-*p*-tosyl-L-lysinechloro-methyl ketone, 50 μg/ml phenylmethylsulfonyl fluoride, 100 μg/ml *N*-tosyl-L-phenylaline chloromethyl ketone, and 1% vol/vol Nonidet P-40]. The extract was cleared by centrifugation at 40,000 *g* for 10 min and the supernatant aliquoted and stored at −80°C. Homogenate protein was quantitated using a commercial assay (Bio-Rad, Richmond, CA) with bovine serum albumin as a reference standard. Samples were separated by size on 7.5% polyacrylamide gels under denaturing conditions as described (13) and electroblotted to nitrocellulose (Hoefer Scientific, San Francisco, CA) membranes in Towbin buffer at 32 V constant voltage (20). The filters were stained with 0.1% napthol blue-black in 45% methanol, 10% acetic acid to assess the efficiency of transfer. Nonspecific binding was blocked by incubation in block buffer (5% nonfat dry milk, 3% bovine serum albumin, 0.1% Tween, 1 × PBS) for 2 h at room temperature. The antibodies used in this study were anti-pRB (no. 14001A; Pharmingen, San Diego, CA), anticyclin (CYC) D1 (no. sc-450), anti-CYC D3 (no. sc-182), anticyclin-dependent kinase (CDK)-4 (no. sc-260), and antiproliferating cell nuclear antigen (PCNA) (no. sc-056; all from Santa Cruz Biotech, Santa Cruz, CA). The TSC2 antibody was provided by Ralf Wienecke (see Ref. 23). In all cases, signal was visualized by the enhanced chemiluminescence method according to the manufacturer's protocol (Amersham).

RESULTS

The temporal pattern of cardiomyocyte DNA synthesis was monitored during murine development by tritiated thymidine incorporation. Mice received a single injection of isotope and were killed 2 h later. The hearts were harvested and isolated cell preparations were generated by collagenase digestion. The isolated cell preparations were then fixed in Formalin and smeared onto microscope slides. Cardiomyocyte labeling indexes were determined by autoradiography followed by microscopic examination (see Ref. 19 for examples). Using this approach, we readily distinguished cardiomyocytes from fibroblasts by virtue of their cellular morphology. The cardiomyocyte labeling index was monitored from embryonic *day 12* through neonatal *day 20;* a total of 21 different time points were analyzed (Fig. 1*A*, Table 1). Although very high cardiomyocyte labeling indexes were detected in early fetal life, the levels of DNA synthesis dropped dramatically at birth (gestation was 20–21 days in the C3HeB/FeJ mice used in this study). A second wave of cardiomyocyte DNA synthesis was observed in early neonatal life, with a peak labeling index of ~10% occurring at neonatal *day 4.6* (Fig. 1*A*). The cardiomyocyte labeling index dropped to 0% by neonatal *day 10,* and no subsequent evidence for cardiomyocyte DNA synthesis was detected (Fig. 1). Importantly, the data presented in Fig. 1 were compiled from two independent experiments performed a year apart; as can be seen the data from the two studies were essentially superimposable.

The biphasic pattern of cardiomyocyte DNA synthesis was not anticipated, because previous studies have suggested that DNA synthesis gradually tapers off during neonatal life, culminating with the appearance of binucleated cells (2, 4, 17). We therefore sought to monitor any developmental changes of cardiomyocyte morphology in light of the observed temporal pattern of DNA synthesis. To ascertain the cardiomyocyte binucleation index, slides of isolated cell preparations were stained with DAPI and visualized under fluorescent illumination. Essentially no cardiomyocyte binucleation was detected during fetal life. However, ~5% of the cardiomyocytes were binucleated by neonatal *day 1.* A dramatic increase in cardiomyocyte binucleation occurred during neonatal *days 4–7* (Fig. 1*A*, Table 1). This increase in binucleation was coincident with the

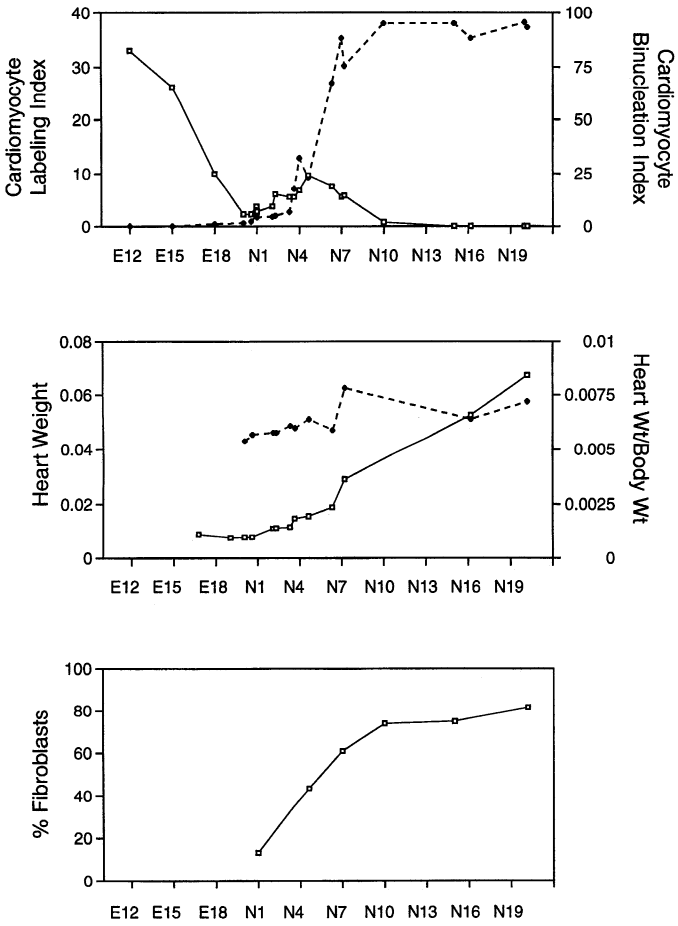

Fig. 1. Cardiomyocyte DNA synthesis, cardiomyocyte binucleation, and cardiac fibroblast content during murine development. *Top:* cardiomyocyte labeling index (left *Y*-axis; □) vs. age during murine development. Labeling index was determined via autoradiography of isolated cell preparations. Also shown is cardiomyocyte binucleation index (right *Y*-axis; ●), which was determined via 4′,6-diamidino-2-phenylindole immunofluorescence assay of isolated cells. *Middle:* absolute heart weight (left *Y*-axis; □) and (heart weight/body weight) × 1,000 ratio (right *Y*-axis; ●) vs. age during murine development. *Bottom:* fibroblast content (% of total cells) vs. age during murine development. E, embryonic day; N, neonatal day.

second phase of cardiomyocyte DNA synthesis. By neonatal *day 10,* the cardiomyocyte binucleation index had reached adult levels. Several other parameters were also monitored during this study. Heart weight increased steadily from embryonic *day 18* to neonatal *day 20,* consistent with the marked myocardial hypertrophy that occurs during neonatal life. In contrast, the heart-to-body weight ratio remained remarkably constant (Fig. 1*B*). Cardiac fibroblast content increased steadily from neonatal *days 1* to *10.* Thereafter the cardiac fibroblast content remained constant (Fig. 1*C*).

The observed labeling and binucleation indexes were consistent with the notion that cardiomyocyte DNA synthesis during fetal life contributed to proliferation (i.e., reduplication), whereas cardiomyocyte DNA synthesis in neonatal life contributed to binucleation. A series of pulse-chase experiments were performed to directly test this hypothesis. A group of neonatal *day 4* mice were given a single injection of tritiated thymidine and killed 48 h later. Isolated cell preparations were generated and subjected to autoradiographic analysis. At the end of the chase period (n = 400 cells) 93.75 ± 0.75% of the autoradiographic signal was localized in binucleated cardiomyocytes. Similarly, in mice injected with tritiated thymidine at neonatal *day 6* and chased to neonatal *day 8,* 90.5 ± 1.52% of the label was localized in binucleated cardiomyocytes (n = 400 cells).

These results support the hypothesis that DNA synthesis in neonatal cardiomyocytes contributes predominately to binucleation. A direct corollary of this hypothesis is that cardiomyocyte reduplication ceases in fetal life, despite the fact that neonatal cardiomyocytes retain the ability to synthesize DNA for binucleation. In contrast, DNA synthesis in fetal cardiomyocytes contributes to reduplication. From these observations one would predict that gene products that impact on cardiomyocyte cell cycle regulation would be differentially expressed during these phases of fetal versus neonatal life. In contrast, nonregulatory gene products required for DNA synthesis and karyokinesis would likely be expressed during both phases. The observation that cardiac fibroblasts comprise only a small percentage of the cells present in early neonatal hearts (Fig. 1, Table 1) suggests that differences in the expression of these putative cardiomyocyte cell cycle regulatory genes would be detectable in total heart preparations from the appropriate stages of development.

Accordingly, expression of several candidate cell cycle regulatory genes was examined during cardiomyocyte reduplication and binucleation. Western blot analyses were performed using total heart protein isolated from embryonic *day 12* to neonatal *day 20* (Fig. 2). Most of the candidate proteins examined (CYCD1, CYCD3, CDK4, and PCNA) exhibited similar levels of expression during fetal life (cardiomyocyte reduplication) and neonatal life (cardiomyocyte binucleation). This temporal pattern of expression was consistent with a generic role in DNA synthesis, based on the paradigm raised above. Expression of the retinoblastoma gene product (pRB) was also monitored. No dramatic shifts in the steady-state levels of pRB were detected in fetal versus neonatal hearts. Moreover, the relative phosphorylation status of myocardial pRB was constant at all stages examined. It should also be noted that the relative level of pRB in the fetal myocardium is ~30-fold lower than in fetal liver (Fig. 2; see also Ref. 11), an organ with pronounced phenotypic anomalies in pRB-deficient mice (3, 8, 14). Collectively, these observations argue against a role for pRB in cardiomyocyte terminal differentiation.

Northern blot analyses were used to monitor the expression of several additional candidate genes. RNA prepared from embryonic *day 12*–neonatal *day 20* hearts was hybridized with cDNA probes from the murine p107, p53, Gax, and TSC2 genes. The levels of expression of p107 and p53 (two of the T-Ag binding proteins identified previously in transgenic cardiomyocyte cell lines) also appeared to closely parallel the relative level of cardiomyocyte DNA synthesis (Fig. 3). In contrast, the Gax (see Ref. 6) gene was not expressed at appreciable levels in mRNA from embryonic *days 12*

Table 1. *Cardiomyocyte DNA synthesis, cardiomyocyte binucleation, and cardiac fibroblast content during murine development*

Day	CM Labeling Index, %	CM Binucleation Index, %	Fibroblast Content, %	Heart Weight, mg	Body Weight, g	HW/BW, mg/g
E 12	33.0 ± 2.12	0	ND	ND	ND	ND
E 15	26.3 ± 0.75	0	ND	ND	ND	ND
E 18	10.0 ± 0.70	1.0 ± 0.41	ND	ND	ND	ND
N 0.04	2.3 ± 0.63	1.5 ± 0.29	ND	7.7 ± 0.46	1.4 ± 0.08	5.4 ± 0.24
N 0.58	2.3 ± 0.48	1.3 ± 0.25	ND	7.7 ± 0.54	1.4 ± 0.04	5.7 ± 0.32
N 0.96	3.8 ± 1.11	5.3 ± 0.25	ND	ND	ND	ND
N 1.0	2.8 ± 0.85	4.3 ± 0.75	13.3 ± 0.75	ND	ND	ND
N 2.1	3.8 ± 0.75	4.5 ± 0.5	ND	11.2 ± 0.35	2.0 ± 0.08	5.8 ± 0.26
N 2.29	6.0 ± 0.41	5.0 ± 1.22	ND	11.3 ± 0.58	2.0 ± 0.04	5.8 ± 0.21
N 3.29	5.5 ± 0.65	6.8 ± 0.75	19.0 ± 4.08	11.7 ± 0.83	1.9 ± 0.12	6.2 ± 0.52
N 3.63	5.5 ± 1.04	17.5 ± 1.19	ND	14.9 ± 0.61	2.5 ± 0.10	6.1 ± 0.57
N 4	6.8 ± 0.48	32.2 ± 1.55	ND	ND	ND	ND
N 4.63	9.8 ± 1.03	23.0 ± 1.78	43.8 ± 1.55	15.7 ± 0.99	2.4 ± 0.08	6.6 ± 0.61
N 6.33	7.5 ± 0.65	67.5 ± 1.88	ND	18.9 ± 1.04	3.2 ± 0.17	5.8 ± 0.36
N 7	5.5 ± 1.44	88.3 ± 2.17	61.0 ± 2.61	ND	ND	ND
N 7.2	5.8 ± 1.03	75.5 ± 1.55	ND	29.0 ± 0.57	3.7 ± 0.12	7.9 ± 0.37
N 10	0.8 ± 0.48	95.0 ± 0.71	73.8 ± 2.46	ND	ND	ND
N 15	0	95.0 ± 1.08	74.8 ± 6.57	ND	ND	ND
N 16.17	0	88.3 ± 1.31	ND	52.7 ± 2.63	8.3 ± 0.28	6.4 ± 0.28
N 20	0	95.5 ± 0.65	81.8 ± 3.35	ND	ND	ND
N 20.20	0	93.3 ± 0.85	ND	67.0 ± 0.86	9.2 ± 0.12	7.3 ± 0.12
Adult	0	91.5	85.8 ± 3.04	ND	ND	ND

Values are means ± SE. E, embryonic; N, neonatal; CM, cardiomyocyte; HW, heart weight; BW, body weight; ND, not determined.

and *15* mice. Expression was markedly induced by embryonic *day 18* and remained at high levels throughout the neonatal period and into adult life (Fig. 3). Expression of the TSC2 (see Refs. 5 and 10) gene was also inversely proportional to cardiomyocyte reduplication. TSC2 was expressed at low levels at embryonic *day 12,* and transcript levels increased progressively as the cardiomyocyte reduplication rate decreased. TSC2 expression reached a maximum level at birth and remained at that level throughout neonatal and adult life.

Given the small size of the fetal hearts examined in this study, it was a formal possibility that noncardiac tissue might inadvertently have been dissected and included in the RNA preparations. Therefore, an additional Northern blot was performed to control for the myocardial content of the early fetal heart RNA samples. The ANF gene is expressed in fetal atria and ventricles and as such provides a good indicator for myocardial

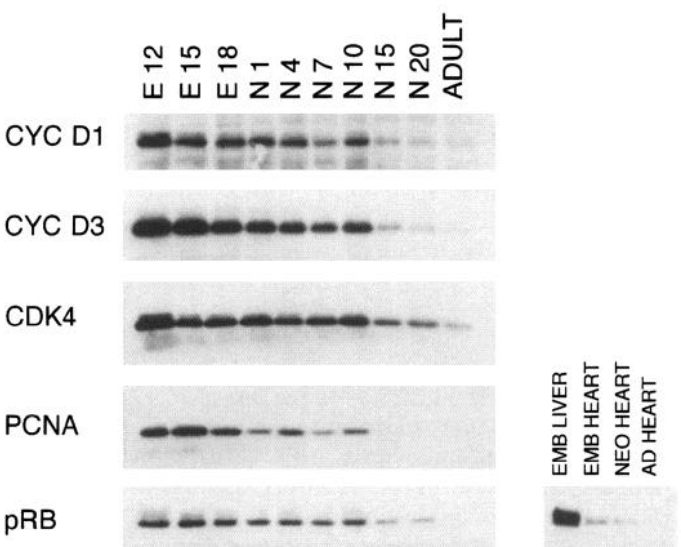

Fig. 2. Western blot analysis of candidate gene expression during myocardial development. Total heart protein was isolated from various stages of development and reacted with antibodies against cyclin (CYC) D1, CYC D3, CDK4, proliferating cell nuclear antigen (PCNA), and retinoblastoma gene product (pRB). Emb, embryonic; neo, neonatal; ad, adult.

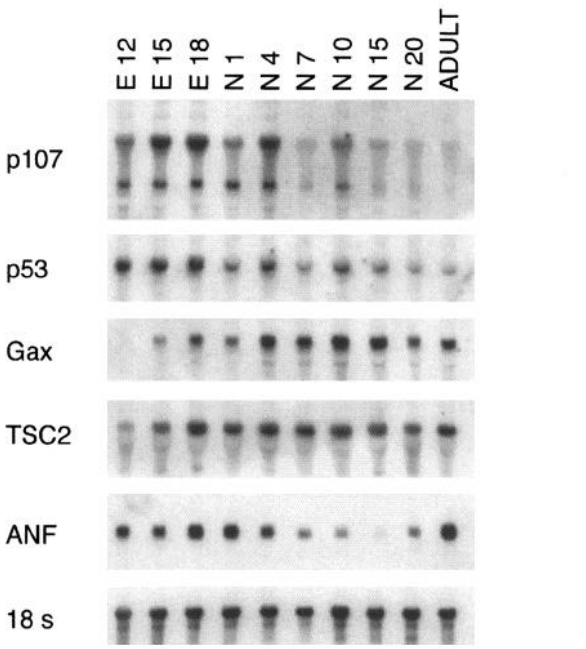

Fig. 3. Northern blot analysis of candidate gene expression during myocardial development. Total heart RNA was isolated from various stages of development and hybridized with radiolabeled probes from the mouse p107, p53, growth-arrest specific homeobox (Gax), tuberous sclerosis complex 2 (TSC2), atrial natriuretic factor (ANF), and 18 s rRNA genes.

content during this stage of development (24). Accordingly, the same RNA samples used to monitor Gax and TSC2 expression were hybridized with an ANF probe. Similar levels of ANF transcripts were detected in samples prepared from embryonic *day 12* to neonatal *day 1* hearts (Fig. 3), indicating that the myocardial content of these samples was comparable. The decreased ANF signal observed in neonatal life was consistent with the restriction of ventricular ANF expression occurring at this stage of development (24). As a final control, the blots were also rehybridized with an 18s rRNA oligonucleotide to confirm the quantity and quality of the RNA samples (Fig. 3).

Additional Western blots were performed to monitor the relative levels of Gax and TSC2 protein. As can be seen, Gax protein levels paralleled exactly the pattern observed for its mRNA (Fig. 4*A*). In contrast, preliminary screens with an anti-TSC2 antibody indicated that relatively high levels of TSC2 protein were expressed in the early fetal heart despite low levels of mRNA. Given this apparent discordance between TSC2 mRNA and protein levels, the Northern and Western blots were repeated with fresh heart samples prepared from embryonic *days 12, 15,* and *18* mice. Once again, a marked increase in TSC2 transcript levels was observed between embryonic *days 12* and *18*. Conversely, TSC2 protein levels were essentially constant through this period (Fig. 4*B*).

DISCUSSION

The results presented here indicate that murine cardiomyocyte DNA synthesis occurred in two temporally distinct phases and that the developmental consequence of DNA synthesis in each phase is markedly different. The high levels of DNA synthesis observed during fetal life contributed to cardiomyocyte reduplication, whereas the DNA synthesis in neonatal life contributed to binucleation. These observations suggest that cardiomyocyte reduplication for the most part is complete by birth, despite the fact that the neonatal cells retain the ability to synthesize DNA. Consequently, genes that exhibit different patterns of expression during the reduplication versus binucleation phases of DNA synthesis would be prime candidates for potential regulators of the cardiomyocyte cell cycle.

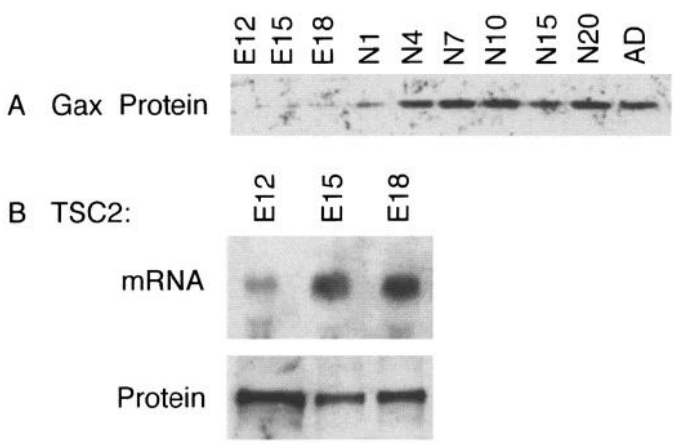

Fig. 4. *A*: Western blot of Gax expression during murine development. Total heart protein was isolated from various stages of development and reacted with antibodies against Gax. *B*: Northern blot analysis (mRNA) and Western blot analyses (protein) of TSC2 in total heart samples prepared from E12, 15, and 18 mice.

Previous studies have demonstrated that cardiomyocyte DNA synthesis gradually tapers off during neonatal life, culminating with the appearance of binucleated cells (2, 4, 17). The data presented here are consistent with these previous studies. However, the labeling indexes reported here were obtained from earlier developmental time points and sampled at more frequent intervals than those reported previously. Thus, although the transient decrease in cardiomyocyte labeling index was detected readily in the present report, retrospective analysis of the earlier studies indicates that the sampling protocols employed would have failed to detect it. Given that the transient decrease in cardiomyocyte labeling index occurred at birth, changes in coronary perfusion, as well as changes in myocardial functional and/or metabolic status, may have influenced the ability to monitor DNA synthesis. However, because the cardiomyocyte nuclear silver grain density was similar at all stages analyzed (M. H. Soonpaa, unpublished observation), and because the decreased labeling index persisted through neonatal *day 2,* it is unlikely that these trivial explanations account for the observed results. A more likely explanation is that the transient decrease in labeling index reflects cessation of cardiomyocyte reduplication before birth in the mouse, and that neonatal DNA synthesis contributes predominately to binucleation. The pulse-chase data reported here as well as in previous studies (2) would tend to support this latter interpretation.

The identification of two temporally and developmentally distinct phases of cardiomyocyte DNA synthesis afforded a unique opportunity to screen for putative regulatory genes. A priori, such genes would be expected to display a differential pattern of expression during the two phases of cardiomyocyte DNA synthesis. As indicated previously, both Gax and TSC2 mRNA were expressed at very low levels during peak cardiomyocyte reduplication and were upregulated during binucleation. Importantly, the steady-state levels of ANF transcripts were constant during these phases of cardiomyocyte development, thereby providing a control for the relative myocardial content in the RNA samples analyzed. This result suggested that the observed increases in Gax and TSC2 mRNA reflected transcriptional induction (or modulation of transcript turnover) as opposed to a sampling artifact.

Both Northern and Western blot analyses indicated that Gax expression was markedly upregulated in the heart during the transition from cardiomyocyte reduplication to binucleation. Gax was originally identified in screens of an adult aorta cDNA library using a probe corresponding to a conserved homeodomain motif (6). Gax expression was observed to be rapidly downregulated in mitogen-stimulated cultures of vascular smooth muscle cells (6) and also during pathophysiological

smooth muscle proliferation after carotid artery balloon injury in vivo (22). Thus Gax expression correlated inversely with smooth muscle proliferation. From this pattern of expression, it is intriguing to note that cardiac Gax expression also correlated inversely with cardiomyocyte proliferation. The notion that Gax may participate in cardiomyocyte cell cycle regulation is bolstered by recent in situ and immunohistochemical data that demonstrated Gax expression in cardiac myocytes at this stage of development (K. Walsh, personal communication).

The situation with TSC2 appears to be somewhat more complicated. Although the steady-state levels of TSC2 transcripts were inversely related to cardiomyocyte reduplication, Western blot analysis suggested a constant level of TSC2 protein throughout all stages of myocardial development examined. This caveat notwithstanding, it is relatively easy to make a case for a potential role for TSC2 in cardiomyocyte cell cycle regulation. Tuberous sclerosis (TS) is a genetically heterogeneous disease characterized by the appearance of nonmalignant growths affecting multiple organ systems, including the heart. Linkage analyses have identified disease-determining loci at 9q34 (TSC1) and 16p13.3 (TSC2; see Ref. 15); the clinical sequelae arising from either genetic lesion are identical. The disease-determining gene on human chromosome 16 (5) as well as the mouse homologue (10) have recently been cloned and characterized. Sequence analysis of cDNA clones revealed that TSC2 encodes a protein (designated tuberin) with a deduced molecular mass of 198 kDa in humans and 202 kDa in mice. Familial TS exhibits an autosomal dominant pattern of inheritance, suggesting that tuberin may function as a tumor suppressor. The loss of heterozygosity at 16p13.3 in some affected tissues from TSC patients provided direct support for this hypothesis (7). The prevalence of primary myocardial tumors in TS patients (21) is also consistent with a regulatory role for tuberin.

In summary, murine cardiomyocyte DNA synthesis occurs in temporally and developmentally distinct phases. Fetal cardiomyocyte DNA synthesis is associated with reduplication, whereas neonatal cardiomyocyte DNA synthesis is associated with binucleation. Northern and Western blot analyses identified several candidate genes that are expressed during the phases of cardiomyocyte reduplication and binucleation, suggestive of a mechanistic role in DNA synthesis and/or karyokinesis. In contrast, other gene products were differentially expressed during these two stages of development, suggesting a potential regulatory role. This assay should provide a useful tool to identify putative cardiomyocyte cell cycle regulatory proteins.

We thank Shaoliang Jing and He Wang for excellent technical assistance, and Drs. Hidehiro Nakajima, Hisako Nakajima, and Michael Klug for comments on the manuscript. We also thank Drs. Rolf Wienecke and Jeff DeClue (National Cancer Institute) for the anti-TSC2 antibody, and Drs. Ken Walsh and Roy Smith (St. Elizabeth's Medical Center) for the ultimate level of assistance with the Gax Western blot.

This work was supported by National Heart, Lung, and Blood Institute Grants HL-45453 and HL-06308 and was done during the tenure of an Established Investigatorship from the American Heart Association (to L. J. Field).

Address for reprint requests: L. J. Field, Krannert Institute of Cardiology, 1111 W. 10th St., Indianapolis, IN 46202-4800.

Received 16 April 1996; accepted in final form 22 August 1996.

REFERENCES

1. **Argentin, S., M. Nemer, J. Drouin, G. K. Scott, B. P. Kennedy, and P. L. Davies.** The gene for rat atrial natriuretic factor. *J. Biol. Chem.* 260: 4568–4571, 1985.
2. **Brodsky, W. Y., A. M. Arefyeva, and I. V. Uryvaeva.** Mitotic polyploidization of mouse heart myocytes during the first postnatal week. *Cell Tissue Res.* 210: 133–144, 1980.
3. **Clarke, A. R., E. R. Maandag, M. van Roon, N. M. van der Lugt, M. van der Valk, M. L. Hooper, A. Berns, and H. te Riele.** Requirement for a functional *Rb-1* gene in murine development. *Nature Lond.* 359: 328–330, 1992.
4. **Clubb, F. J., Jr., and S. P. Bishop.** Formation of binucleated myocardial cells in the neonatal rat. An index for growth hypertrophy. *Lab. Invest.* 50: 571–577, 1984.
5. **European Chromosome 16 Tuberous Sclerosis Consortium.** Identification and characterization of the tuberous sclerosis gene on chromosome 16. *Cell* 75: 1305–1315, 1993.
6. **Gorski, D. H., D. F. LePage, C. V. Patel, N. G. Copeland, N. A. Jenkins, and K. Walsh.** Molecular cloning of a diverged homeobox gene that is rapidly down-regulated during the G0/G1 transition in vascular smooth muscle cells. *Mol. Cell Biol.* 13: 3722–3733, 1993.
7. **Green, A. J., M. Smith, and J. R. Yates.** Loss of heterozygosity on chromosome 16p13.3 in hamartomas from tuberous sclerosis patients. *Nat. Genet.* 6: 193–196, 1994.
8. **Jacks, T., A. Fazeli, E. M. Schmitt, R. T. Bronson, M. A. Goodell, and R. A. Weinberg.** Effects of an Rb mutation in the mouse. *Nature Lond.* 359: 295–300, 1992.
9. **Kellerman, S., J. A. Moore, W. Zierhut, H. G. Zimmer, J. Campbell, and A. M. Gerdes.** Nuclear DNA content and nucleation patterns in rat cardiac myocytes from different models of cardiac hypertrophy. *J. Mol. Cell Cardiol.* 24: 497–505, 1992.
10. **Kim, K. K., L. Pajak, H. Wang, and L. J. Field.** Cloning, developmental expression, and evidence for alternative splicing of the murine tuberous sclerosis (TSC2) gene product. *Cell. Mol. Biol. Res.* 41: 515–526, 1995.
11. **Kim, K. K., M. H. Soonpaa, A. I. Daud, G. Y. Koh, J. S. Kim, and L. J. Field.** Tumor suppressor gene expression during normal and pathologic myocardial growth. *J. Biol. Chem.* 269: 22607–22613, 1994.
12. **Kim, K. K., M. H. Soonpaa, H. Wang, and L. J. Field.** Developmental expression of p107 mRNA and evidence for alternative splicing of the p107 (RBL1) gene product. *Genomics* 28: 520–529, 1995.
13. **Laemmli, U. K.** Cleavage of structural proteins during the assembly of the head of bacteriophage T4. *Nature Lond.* 227: 680–685, 1970.
14. **Lee, E. Y., C. Y. Chang, N. Hu, Y. C. Wang, C. C. Lai, K. Herrup, W. H. Lee, and A. Bradley.** Mice deficient for Rb are nonviable and show defects in neurogenesis and haematopoiesis. *Nature Lond.* 359: 288–294, 1992.
15. **Povey, S., M. W. Burley, J. Attwood, F. Benham, D. Hunt, S. J. Jeremiah, D. Franklin, G. Gillett, S. Malas, and E. B. Robson.** Two loci for tuberous sclerosis: one on 9q34 and one on 16p13. *Ann. Hum. Genet.* 58: 107–127, 1994.
16. **Raynal, F., B. Michot, and J. P. Bachellerie.** Complete nucleotide sequence of mouse *18 S rRNA* gene: comparison with other available homologs. *FEBS Lett.* 167: 263–268, 1984.
17. **Rumyanstev, P. P.** *Growth and Hyperplasia of Cardiac Muscle Cells,* edited by Bruce M. Carlson. New York: Harwood Academic, 1991, p. 70–157.
18. **Sambrook, J., E. F. Fritsch, and T. Maniatis.** *Molecular Cloning.* Cold Spring Harbor, NY: Cold Spring Harbor Laboratory Press, 1989, p. 3v.

19. **Soonpaa, M. H., and L. J. Field.** Assessment of cardiomyocyte DNA synthesis during hypertrophy in adult mice. *Am. J. Physiol.* 266 (*Heart Circ. Physiol.* 35): H1439–H1445, 1994.
20. **Towbin, H., T. Staehelin, and J. Gordon.** Electrophoretic transfer of proteins from polyacrylamide gels to nitrocellulose sheets: procedure and some applications. *Proc. Natl. Acad. Sci. USA* 76: 4350–4354, 1979.
21. **Watson, G. H.** Cardiac rhabdomyomas in tuberous sclerosis. *Ann. NY Acad. Sci.* 615: 50–57, 1991.
22. **Weir, L., D. Chen, C. Pastore, J. M. Isner, and K. Walsh.** Expression of gax, a growth arrest homeobox gene, is rapidly down-regulated in the rat carotid artery during the proliferative response to balloon injury. *J. Biol. Chem.* 270: 5457–5461, 1995.
23. **Wienecke, R., A. Konig, and J. E. DeClue.** Identification of tuberin, the tuberous sclerosis-2 product. Tuberin possesses specific Rap1GAP activity. *J. Biol. Chem.* 270: 16409–16414, 1995.
24. **Zeller, R., K. D. Bloch, B. S. Williams, R. J. Arceci, and C. E. Seidman.** Localized expression of the atrial natriuretic factor gene during cardiac embryogenesis. *Genes & Dev.* 1: 693–698, 1987.